Materials Research Proceedings 28 (2023) 2101-2113 https://doi.org/10.21741/9781644902479-225

Fine blanking of pre-hardened high manganese steel to investigate the sheared surface hardening and part quality

SCHWEINSHAUPT Frank[1,a *], VOIGTS Herman[1,b], HERRIG Tim[1,c] and BERGS Thomas[1,2,d]

[1]Laboratory for Machine Tools and Production Engineering (WZL) of RWTH Aachen University, Campus-Boulevard 30, 52074 Aachen, Germany

[2]Fraunhofer Institute for Production Technology IPT, Steinbachstraße 17, 52074 Aachen, Germany

[a]f.schweinshaupt@wzl.rwth-aachen.de, [b]H.Voigts@wzl.rwth-aachen.de, [c]T.Herrig@wzl.rwth-aachen.de, [d]t.bergs@wzl.rwth-aachen.de

Keywords: Fine Blanking, High Manganese Steel, Strain Hardening, Twinning Induced Plasticity, Die Roll, Sheared Part Quality

Abstract. Fine blanking is a highly productive process for manufacturing of high accuracy sheet metal parts with functional surfaces. The specific process characteristic leads to high forming in the shear zone and an associated strain hardening of the sheared functional surfaces. Utilization of the process-immanent sheared surface hardening can reduce time and resources of downstream heat treatment processes such as case hardening. High Manganese Steels (HMnS) are characterized by a high strain hardening capacity due to the deformation mechanisms of twinning and transformation induced plasticity occurring during forming. As a result of high tensile strengths, HMnS are suitable as lightweight materials, but often exhibit a relatively low yield strength in terms of structural design features. One approach for increasing the strength values without changing the alloy design is a forming-induced strain hardening of the semi-finished sheet metal by means of upsetting. Therefore, this paper deals with an experimental investigation of the influence of pre-hardening on the blanked part properties during fine blanking of HMnS X40MnCrAlV19-2 LY (1.7401). For this purpose, sheet blanks were strain hardened by means of flat coining and subsequently fine blanked with an analog geometry representing tribologically stressed functional surfaces. Relevant functional surfaces were then analyzed by means of microhardness measurements with regard to the sheared surface hardening as well as characterized in terms of the quality-determining attributes die roll and clean-shear area. Due to the deformation mechanism of twinning, fine blanking of pre-hardened HMnS resulted in a combination of process-immanent high sheared surface hardening and increased yield strength with simultaneous optimal functional surface quality.

Introduction

The intrinsically driven economic resource efficiency [1] as well as the reduction of ecologically harmful emissions [2] force a continuous optimization of product development and the necessary manufacturing processes in the sheet metal processing industry. Particularly in the development of dynamically moving sheet metal workpieces, this results in the implementation of consistent lightweight design strategies for saving raw materials and emissions through lightweight material, shape and concept design [3]. Fine blanking is a process for the series production of geometrically complex sheet metal workpieces with high dimensional and shape accuracy combined with optimum material utilization [4]. Due to the high accuracy and quality of the sheared surface, fine blanking is a near-net-shape technology, e.g. for the manufacturing of gears or sprockets [5]. Process characteristics of fine blanking (cf. Fig. 1b and c) are three independently acting process forces (blanking, counter and vee-ring force), a small relative die clearance, a wedge-shaped vee-

ring as well as die edges prepared with a chamfer or radius [6]. During the shearing process, the vee-ring and counter force induce a high hydrostatic pressure in the shear zone [7]. The embossing of the vee-ring, the die edge preparation as well as a small die clearance favor the formation of additional compressive stresses [8]. The resulting superimposed compressive stress generates a plastic flow in the shear zone over the entire blanking path, which prevents tensile stresses and results in a smooth and tear-free sheared surface of high quality [9]. The load-bearing capacity of sheared functional surfaces is reduced by a die roll (cf. Fig. 1c), which is completely formed after 20 to 30% of the blanking path [10]. A large number of scientific studies have already investigated the factors influencing the clean-shear area and die roll during fine blanking and have shown comparable tendencies regarding the influence of process (e.g. vee-ring force), tool (e.g. die clearance) and workpiece parameters (e.g. material properties) [7].

In terms of process mechanics, a small die clearance with increasing blanking velocity from 10 to 70 mm/s causes a significant temperature increase of the shear zone during plastic flow as well as an increase of the blanking force [11]. The plastic flow of the sheet material in the shear zone basically leads to high deformation in the area in front of the die edge, which results in a significant increase in the dislocation density and thus in strain hardening of the sheared surface [12]. This process-immanent hardening in the near-surface area of fine blanked functional surfaces offers the potential to substitute a downstream heat treatment by using sheet materials with high strengths and strain hardening properties [8]. Regarding the use of lightweight materials, High Strength Steels (HSS) such as micro-alloyed fine grain steel S700MC (1.8974) are increasingly used for fine blanking [13]. However, as increasing strength is accompanied by a lower forming capacity [14], HSS are only suitable to a limited extent for forming sheet metal workpieces with spatially complex geometry. High Manganese Steels (HMnS) exhibit a superior combination of high strength and high formability [15] and thus offer the potential to address both lightweight material and shape design in sheet metal workpieces. HMnS are classified with a manganese content higher than 15 wt.% and characterized by a high strain hardening capacity during plastic deformation [16]. Forming of HMnS thus leads to a high strain hardening of the plasticized area, which is a result of the occurring secondary deformation mechanisms Twinning Induced Plasticity (TWIP) and Transformation Induced Plasticity (TRIP). With unchanging alloy design, the activation of different deformation mechanisms and thus the influence on the hardening behavior depends on the temperature [17], stress state [18] and strain rate [19]. The alloy design of a HMnS influences the magnitude of the stacking fault energy (SFE), which is used as a parameter to adjust the secondary deformation mechanism [16]. This enables the design of a specific deformation mechanism at a given temperature based on thermodynamic calculations of the SFE [20]. Despite the high strain hardening capacity, HMnS often exhibit low yield strength due to the soft austenitic matrix [17].

However, in order to exploit a lightweight and forming potential based on deformation mechanisms in fine blanking of HMnS, fundamental investigations are still lacking. Investigations on fine blanked sprockets made of non-alloy structural steel S275JR (SS400) have shown that these exhibit a higher wear resistance due to the sheared surface hardening than conventionally manufactured and heat-treated sprockets made of non-alloy quenched and tempered steel C50 (S50C) [21]. As a result of increased residual compressive stresses, fine blanked gears made of micro-alloyed fine grain steel S355MC (1.0976) showed a comparably high tooth root bending strength to low-alloy, heat-treated case-hardening steels [22]. Fine blanking of higher-strength Dual Phase (DP) steels DP600 [23] as well as DP780 and DP980 [24] offers potential for substitution of downstream heat treatment due to the strain hardening behavior, but also resulted in poor sheared surface quality with a tear-off height of more than 50% of the sheet thickness. Investigations on fine blanking of TRIP steel also revealed large tear-off heights of 40% of the sheet thickness at the sheared surfaces [25]. In a study on fine blanking of flat coined case-

hardening steel 16MnCr5 (1.7131), the die roll formation was reduced due to a forming-induced increase in the strength values [26].
In fine blanking of conventional steels, the sheared surface hardening has a positive effect on the behavior of tribologically stressed functional surfaces and thus shows potential for substituting heat treatment. The high deformation in the area in front of the die edge provides an ideal condition for utilizing the combination of high strain hardening and high formability during fine blanking of HMnS. Pre-hardening of the sheet material by means of upsetting represents a possible approach for influencing the strength values of HMnS. In order to achieve a combination of increased yield strength and high sheared surface hardening, fine blanking of pre-hardened HMnS was investigated in the present work. For this purpose, sheet metal blanks with various height reductions have been flat coined and fine blanked with a part geometry representing tribologically stressed functional surfaces. Depending on the part geometry, an analysis of the strain hardening as well as quality-determining attributes was then carried out.

Experimental Setup for Fine Blanking of Pre-Hardened HMnS

To investigate the influence of pre-hardened HMnS on the sheared part properties during fine blanking, sheet blanks made of hot-rolled X40MnCrAlV19-2 LY (1.7401) with the dimensions given in Fig. 1a were used. In order to evaluate the potential of mechanism-induced sheared surface hardening, additional sheet blanks of micro-alloyed fine grain steel S700MC (1.8974) have been fine blanked. Table 1 shows the yield strength $R_{\mathrm{p0.2}}$, ultimate tensile strength R_{m}, uniform elongation A_{G}, elongation at fracture A and initial hardness for the sheet materials.

Table 1. Characteristic values of the mechanical properties valid for room temperature T = 22°C

Material	$R_{\mathrm{p0.2}}$ [MPa]	R_{m} [MPa]	A_{G} [%]	A [%]	Initial hardness [HV0.1]
HMnS	407	843	50	A_{50} = 55	202 ±4
S700MC	780	865	9.5	A_{80} = 19.1	296 ±5

Fig. 1a and b show the schematic setup for fine blanking of pre-hardened HMnS. The pre-hardening of the sheet blanks was carried out in a tool for flat coining with two parallel ground upset plates. The tool-side adjustment of the height reductions Δs_i was carried out using spacers adapted to the target sheet thickness of s = 4.6 mm. In order to investigate two different pre-hardening stages of HMnS, sheet blanks have been surface ground on both sides to the initial sheet thicknesses $s_{\mathrm{I}i}$ specified in Fig. 1a. As a reference for the sheared part analysis, sheet blanks from both HMnS and S700MC were additionally surface ground to the target sheet thickness of s = 4.6 mm.

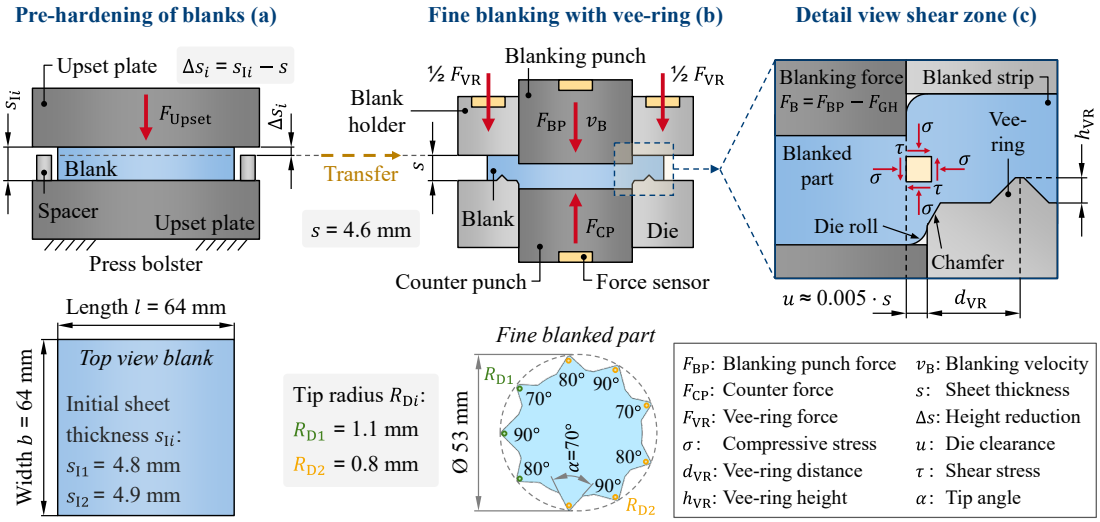

Fig. 1. Setup for pre-hardening (a) with subsequent fine blanking (b) and a detailed view of the shear zone (c).

Flat coining was carried out on a *Schuler HPX 400* hydraulic press with a ram velocity of 5 mm/s. After measuring the upset sheet blanks regarding the height reduction, the fine blanking tests were conducted on a servomechanical fine blanking press *Feintool XFT 2500 speed*. Fine blanking was performed with a modular designed single part producing tool (one part per stroke), which is instrumented with piezoelectric force sensors to measure the process forces. The sheared part geometry consisting of convex form elements with different tip angles α and tip radii R_{Di} represents an analogy application case for tribologically stressed functional surfaces. Acute angles with small radii are challenging (high difficulty level D) in terms of blanked part quality as well as punch edge load. To categorize the difficulty level, classification tables dependent on the sheet thickness and sheared part geometry (e.g. angles) are used according to [8], where $D = 1$ represents the lowest difficulty. The major geometric quantities of the sheared part are shown in Fig. 1b. The blanking punch and die were manufactured from *Böhler S390* powder metallurgical high speed steel with a hardness of 65 HRC and provided with the *Platit FeinAl* coating (AlCrN-based nanolayer coating) tailored to fine blanking. *Holifa VP1150/200* chlorine-free lubricant was used for the flat coining and fine blanking experiments. The process and tool parameters used for fine blanking are specified in Table 2.

Table 2. Process and tool parameters used for fine blanking.

Blanking velocity v_B	45 mm/s	**Die chamfer angle**	35°
Vee-ring force F_{VR}	620 kN	**Die chamfer height**	0.3 mm
Counter force F_{CP}	170 kN	**Vee-ring distance d_{VR}**	2.5 mm
Die clearance u	20 µm	**Vee-ring height h_{VR}**	0.7 mm

In order to investigate the mechanical properties and to evaluate the hardening behavior, tensile tests of the HMnS used were conducted at the *Steel Institute IEHK* according to DIN EN ISO 6892. The tensile tests were carried out at different temperatures using a *ZwickRoell Z250* tensile testing machine with a temperature chamber. The strain was measured in an open loop using *Zwick multiXtens*. Dynamic tensile tests were conducted at a strain rate of 10 /s using a servohydraulic 20kN *Roell-Amsler* high-speed (18m/s) tensile testing machine. The force was measured by a piezo

electric load cell and combined with strain gauges on the sample heads to obtain a smoothed signal [27]. The initial dimensions of the samples used had a thickness of 2mm, length of 15mm and width of 6mm. The analysis of the sheared surface hardening was carried out in dependence of the part geometry using the three convex form elements with the tip radius R_{D1} = 1.1 mm (Fig. 2a). For this purpose, samples at the corresponding tip angles α were separated out for each blanked part investigated in such a way that the separation line A-A is aligned normally to the functional surface. After metallographic preparation, microhardness measurements were conducted according to the scheme shown in Fig. 2.

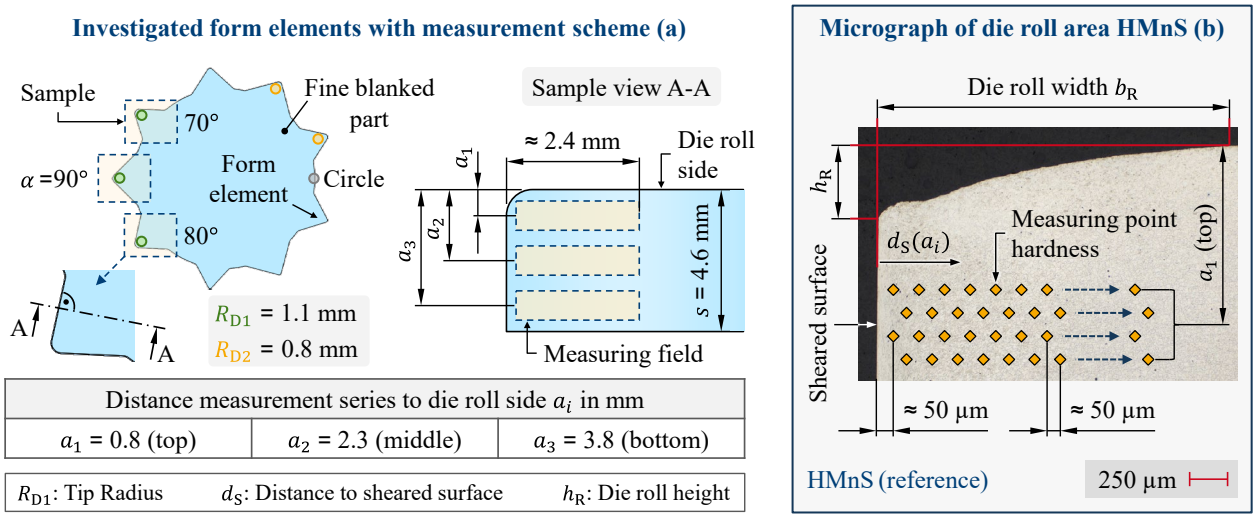

Fig. 2. Investigated form elements with measurement scheme (a) and a micrograph of the die roll area (b).

Since the sheared surface hardening depends on the blanking path, three measuring fields were investigated based on the distance to the die roll side a_i. Fig. 2b exemplarily shows a micrograph of the die roll area of HMnS at the position circle with the pattern of hardness indentations, which have horizontally as well as vertically an indentation distance of 100 µm to each other. The high strain hardening directly below the sheared surface enables the hardness measurement to start at a distance of 50 µm from it. To increase the resolution of the hardness profile, an associated series of measurements was carried out with an offset of half an indentation distance. In order to enable a smoothing of the hardness values by means of averaging, two of these patterns were measured for each measuring field. The microhardness measurements were done using a *Fischer* microhardness measuring system *Fischerscope HM2000* according to the force-indentation depth method with a holding time of 10 s. In this case, the Vickers hardness *HV* is determined by converting the plastic part of the universal hardness HU_{pl} based on DIN 50359-1 into HV_{pl}. In order to evaluate the quality-determining attributes of fine blanking, the die roll was measured and the functional surfaces were investigated regarding tear-off. To determine the die roll, the fine-blanked parts were polygonized using a *GOM ATOS Core 3D* scanner and a software-based target-actual comparison was conducted using a CAD model by means of *GOM Inspect Suite*. For this purpose, the height differences at the form elements marked with colored circles in Fig. 2a were measured in a 2D plot using sectional planes with an equidistant step size of 2.5 µm and evaluated script-based. For the investigation of the tear-off height, images of the functional surfaces were taken based on light optical microscopy (LOM) using a *Keyence VHX-5000* digital microscope and evaluated graphically. For each analyzed state regarding the pre-hardening of the HMnS as well as the additionally considered HSS S700MC, respectively two blanked parts were evaluated

and averaged for the hardness results. All other analysis results presented are based on the averaging of five blanked parts in each case.

Results Analysis

To evaluate the strain hardening behavior, Fig. 3a shows the calculated SFE of the investigated HMnS as a function of the temperature as well as the ranges of assumed secondary deformation mechanisms. The SFE was calculated based on a thermodynamic model using the chemical composition of X40MnCrAlV19-2 LY at a grain size of 30 µm [20]. Generally, a SFE below 18 to 20mJ/m^2 enables a TRIP effect and a higher SFE up to about 50mJ/m^2 results in a TWIP effect. [28]. Above an SFE of 45 to 50mJ/m^2, twinning is drastically reduced and dislocation slip (SLIP) is the preferred activated deformation mechanism [16]. For the HMnS investigated, the TWIP effect is assumed to occur in a temperature range of approx. -20 to 140°C.

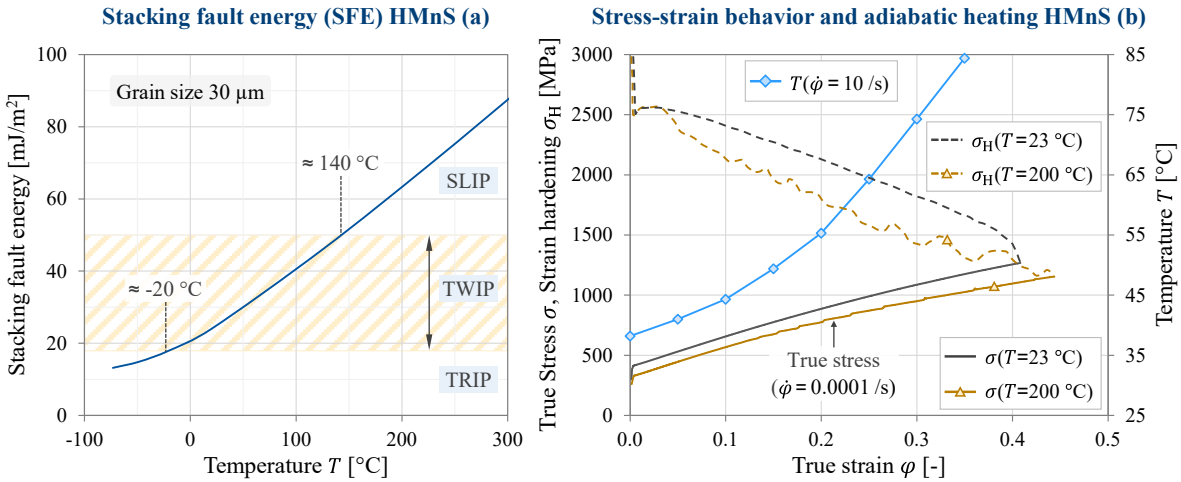

Fig. 3. Calculated SFE (a) and stress-strain behaviour (quasi-static) as well as adiabatic heating (dynamic) (b).

Fig. 3b shows the strain hardening behavior of HMnS based on true stress-strain and strain hardening curves determined from the tensile tests. The true stress-strain curves were determined for a temperature of 23 and 200°C with a strain rate of $\dot{\varphi}$ = 0.0001 /s. The corresponding strain hardening curves shown (dashed lines) result from the derivation of the respective stress-strain curves. An increase in temperature leads to a reduced flow stress in the stress-strain progression. Likewise, the corresponding strain hardening curve is significantly reduced with increasing temperature from a true strain of approx. $\varphi \approx 0.04$. Since the elastic strain of the tool elements in the force flow and the true strain of the sheet material in the shear zone are superimposed during fine blanking, the exact determination of the strain rate is challenging. Neglecting the elastic tool strain, the strain rate with regard to the investigated process parameters is about 10 /s during the shearing process. Fig. 3b additionally shows the temperature rise due to adiabatic heating measured by thermography during the dynamic tensile test for a strain rate of $\dot{\varphi}$ = 10 /s up to a true strain of $\varphi \approx 0.35$. The rising adiabatic heating as well as the reduction in strain hardening at higher temperature during the tensile tests indicate an increase in SFE (Fig. 3a) and thus an influence on the strain hardening behavior due to shearing of HMnS.

Based on the respective initial sheet thickness s_{1i}, the height reductions Δs_i were measured to determine the relative height reduction $\Delta h = \Delta s_i / s_{1i}$ of the upset sheet blanks. For the first pre-hardening stage, a height reduction Δs_1 = 0.2 mm with a deviation of ±0.012 mm was obtained, which corresponds to a relative height reduction of $\Delta h \approx 4.2\%$. With a deviation ±0.015 mm for Δs_2 = 0.3 mm, the relative height reduction for the second pre-hardening stage is $\Delta h \approx 6.1\%$. To

evaluate the process behavior during the shearing process, Fig. 4a shows the blanking force progression of the HMnS in the reference state (Δh = 0%) compared to HSS S700MC and exemplarily the specified vee-ring and counter force. Due to the sensor arrangement (cf. Fig. 1b), the blanking force F_B is determined by subtracting the counter force F_{CP} from the blanking punch force F_{BP}. In the fine blanking press used, the counter and vee-ring force are applied hydraulically and exhibit a subsiding oscillating curve over the shearing phase resulting from the closed loop control behavior. Both force curves are slightly above the set values after transient oscillation, but during the shearing phase the underlying settings are obtained on average.

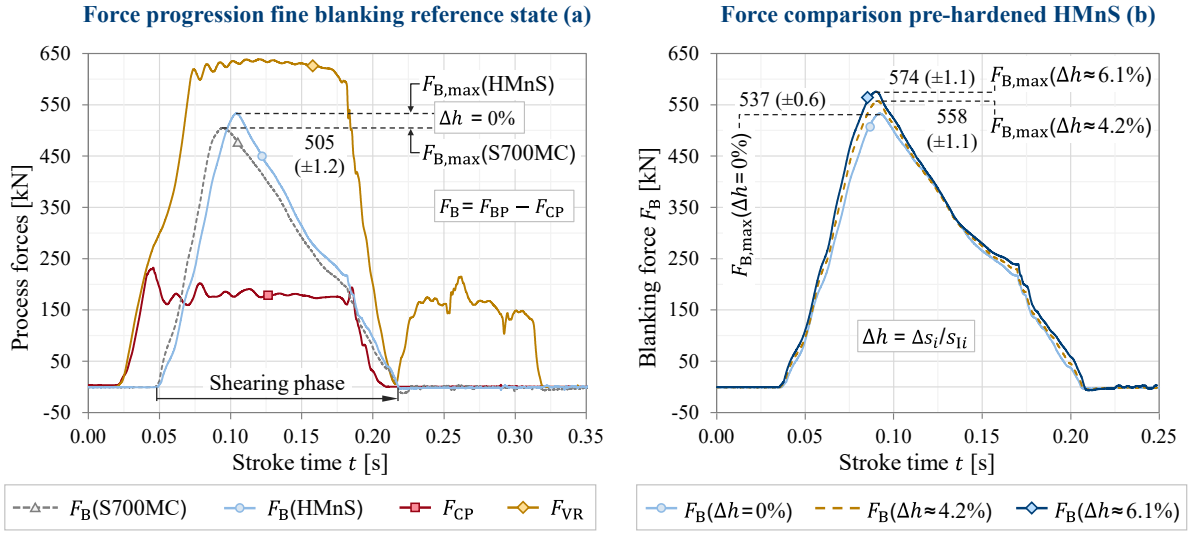

Fig. 4. Fine blanking forces of the reference state (a) and blanking force comparison of pre-hardened HMnS (b).

Despite almost equally high tensile strength compared to the HSS S700MC, an increased maximum blanking force $F_{B,max}$ of approx. 32 kN is observed for the reference state of the HMnS (Fig. 4a) due to the high hardening capacity. The slightly less steep increase in blanking force in the shearing phase is due to the forming behavior of HMnS reflected in the yield strength $R_{p0.2}$. In contrast, the comparison of pre-hardening stages shown in Fig. 4b indicates a more rapidly rising blanking force with increasing relative height reduction Δh, which can be explained by an increase of the yield strength. For the first pre-hardening stage (Δh = 4.2%), the maximum blanking force increases by 21 kN and for the second (Δh = 6.1%) by 37 kN compared to the reference state of HMnS. With less than 0.3%, the standard deviations of the maximum blanking force given in parentheses are to be considered as neglectable.

Fig. 5a shows the sheared surface hardening for fine blanked HMnS in the reference state (Δh = 0%) as well as for HSS S700MC with respect to the functional surface α = 80° for the measuring fields (cf. Fig. 2a) top (a_1) and bottom (a_3). As expected, the hardness values in the near-surface area ($d_S \leq 0.5$ mm) increase related to the die roll side with increasing blanking path (top to bottom). Due to the high strain hardening capacity, the HMnS is characterized in the near-surface area by a pronounced sheared surface hardening with an enormous hardness increase. Directly below the sheared surface, the hardness values of HMnS are approx. 140 HV higher than the values of S700MC for the top as well as the bottom measuring field. The plotted work hardening depth of the respective materials indicates the distance from the sheared surface where the bulk hardness is reached on average regarding the measuring field middle. With a value of about $d_S \approx 1.6$ mm, the HMnS in the reference state (Δh = 0%) achieves a work hardening depth more than twice as large as that of the micro-alloyed fine grain steel. According to DIN EN ISO

18203, the hardness value for determining the case hardening depth CHD is defined as 550 HV, and for determining the surface hardening depth SHD, limiting hardness values are specified based on the minimum surface hardness. For the measuring field bottom, the achieved sheared surface hardening of HMnS is accordingly comparable with a case hardening depth of CHD ≈ 0.15 mm and for a surface hardness ($d_S \approx 0$ mm) of 630 HV with a surface hardening depth of SHD ≈ 0.25 mm.

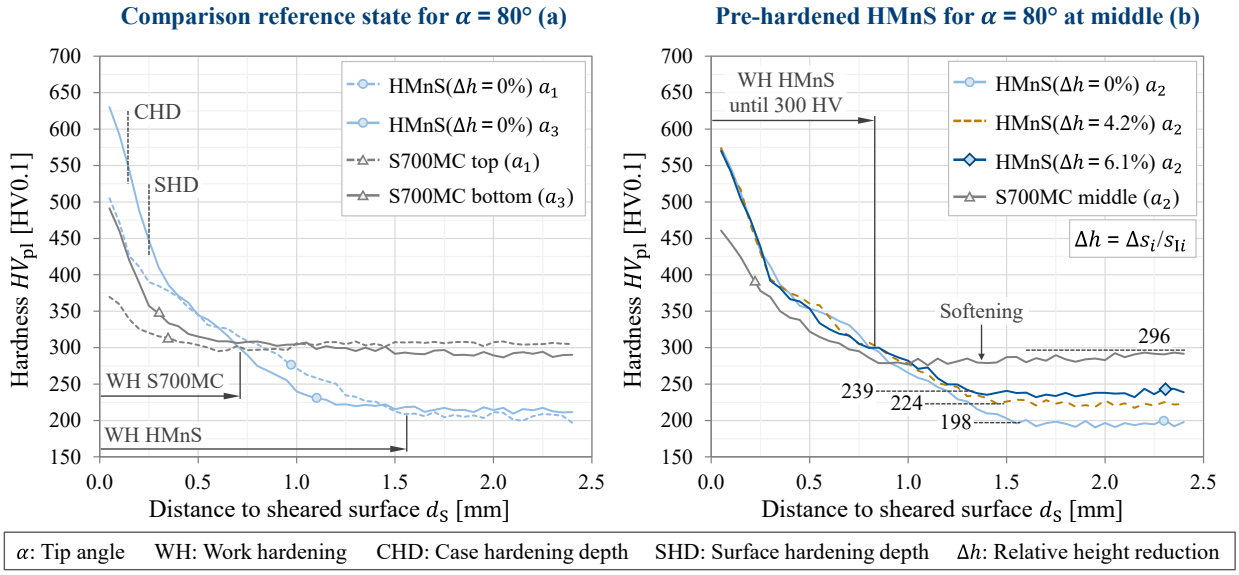

Fig. 5. Sheared surface hardening for tip angle α = 80° regarding the reference state (a) and pre-hardening (b).

Fig. 5b shows the hardening of the fine blanked functional surface α = 80° depending on the relative height reduction Δh carried out for pre-hardening of the HMnS in comparison to the HSS S700MC for the measuring field middle (a_2). The pre-hardening of the HMnS has no influence on the profile and the height of the sheared surface hardening in the near-surface area, but causes an increase in the bulk hardness, of which the averaged value is given for each hardness profile shown. The first pre-hardening stage (Δh = 4.2%) increases the bulk hardness by an average of 26 HV and the second (Δh = 6.1%) by an average of 43 HV, which in each case also suggests an increase in the yield strength. Compared to the measuring field middle, the hardness values for the reference state of the HMnS in the field bottom (Fig. 5a) are above the determined bulk hardness (~198 HV) after reaching the work hardening depth ($d_S \geq 1.6$ mm). One possible reason that the hardness values are on average 14 HV higher than the bulk hardness is a strain hardening due to the induced compressive stresses of the vee-ring and counter force at least in the area of the sheet surface close to the shear zone. The hardness profile for the S700MC in the measuring field middle (Fig. 5b) shows a slight softening with values about 20 HV lower than the bulk hardness (~296 HV) in the range of $d_S \approx 0.8$ to 2.2 mm. With increasing pre-hardening Δh, the achievable work hardening depth of the HMnS decreases (Fig. 5b). Based on a bulk hardness of 300 HV, a work hardening depth of at least $d_S \approx 0.8$ mm is to be expected for the measuring field middle with increasing pre-hardening of the HMnS.

The tip angle of the convex form elements also has no influence on the profile and height of the sheared surface hardening with respect to the investigated tip radius R_{D1} = 1.1 mm. Fig. 6a exemplarily shows the hardness profiles for pre-hardened HMnS (Δh = 6.1%) and S700MC for the measuring field middle (a_2) depending on the tip angle α. The achieved work hardening depth of the second pre-hardening stage of HMnS is about $d_S \approx 1.3$ mm. Regarding a comparison to case

and surface hardening, for the measuring field middle the hardening depths are CHD ≈ 0.1 mm and SHD ≈ 0.2 mm (surface hardness 570 HV). For all determined hardness profiles, the scatter of the averaged hardness values lies within a range of ±6.4 HV.

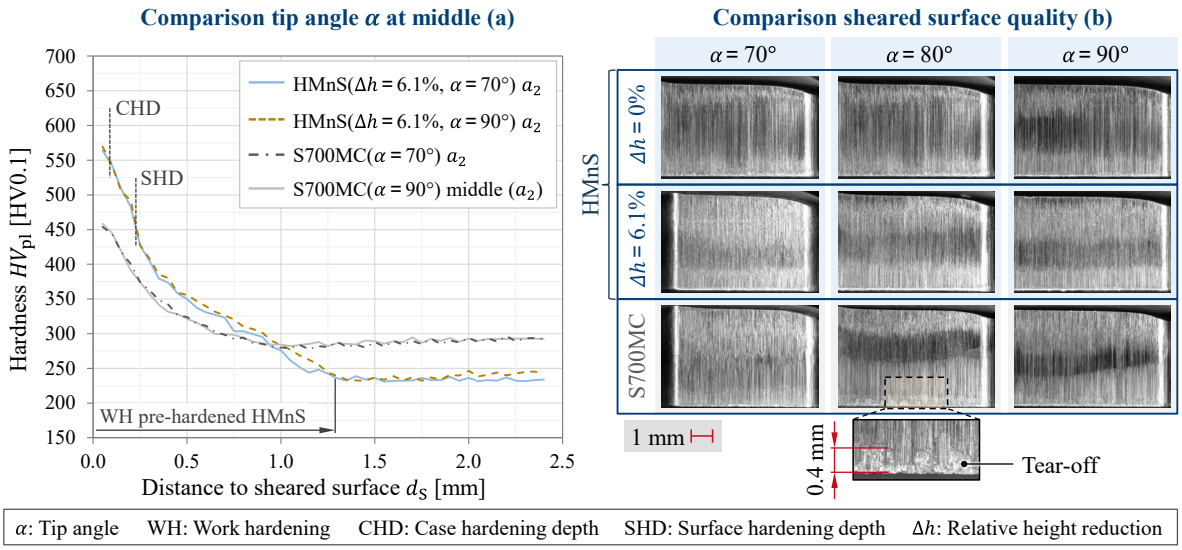

Fig. 6. Sheared surface hardening regarding the tip angle (a) and quality of the functional sheared surfaces (b).

The quality of the investigated functional surfaces is shown in Fig. 6b based on the LOM images for the reference state and the second pre-hardening stage of the HMnS compared to the HSS S700MC. Independent of the investigated tip angle α as well as the relative height reduction Δh, the fine blanked HMnS is characterized by a high sheared surface quality without tears and with tear-off heights below 0.05 mm. The micro-alloyed fine grain steel exhibits a comparably high sheared surface quality with minor tear-off heights of about 0.2 mm at α = 70° and 80° and a tear-off height of 0.4 mm at α = 90°.

For the analysis of the die roll formation, two tip angles with smaller tip radius (R_{D2} = 0.8 mm) were considered in addition to the form elements marked with R_{D1} in Fig. 2a. Fig. 7a shows the characteristics of the investigated fine blanked part and the sectional planes used to measure the die roll. The sectional planes are collinear to the respective angle bisector of the investigated tip angle α. In order to quantify the influence of pre-hardening on die roll formation during fine blanking of HMnS, relative reference values have been formed based on the values of the determined heights and widths. The relative die roll height difference Δh_{PH} indicates the relative reduction between the reference state (Δh = 0%) and the second pre-hardening stage (Δh = 6.1%) of the HMnS and is based on the minimal die roll height difference $\Delta h_{R,min}$ in each case for considering the variation range. The minimal die roll height difference was determined using the standard deviations calculated for the respective worst case (cf. Fig. 7b). The determination of the relative die roll width difference Δb_{PH} regarding the pre-hardening is based on an analogous approach to Δh_{PH}. The evaluation of the HMnS compared to the micro-alloyed fine grain steel is carried out on the basis of the relative die roll height difference Δh_{MF} as well as width difference Δb_{MF}. These reference values indicate the relative difference between the reference state of the HMnS and the HSS S700MC and were determined analogously to the procedure described before. The results of the die roll analysis are shown in Fig. 7b in dependence of the investigated form elements. The pre-hardening of the HMnS results in a reduction of the die roll at all form elements, which rises with increasing relative height reduction Δh. For the HMnS, the second pre-hardening stage results in reductions of about Δh_{PH} ≈ 7 to 11% in terms of the die roll height and about

$\Delta b_{PH} \approx 7$ to 14% in terms of the die roll width. Compared to the HSS S700MC, a larger die roll is formed for the reference state of the HMnS, which is characterized by approx. $\Delta h_{MF} \approx 30$ to 56% higher die roll heights and between $\Delta b_{MF} \approx 50$ to 60% higher die roll widths. For the second pre-hardening stage of HMnS, the relative difference values to S700MC are consequently lower.

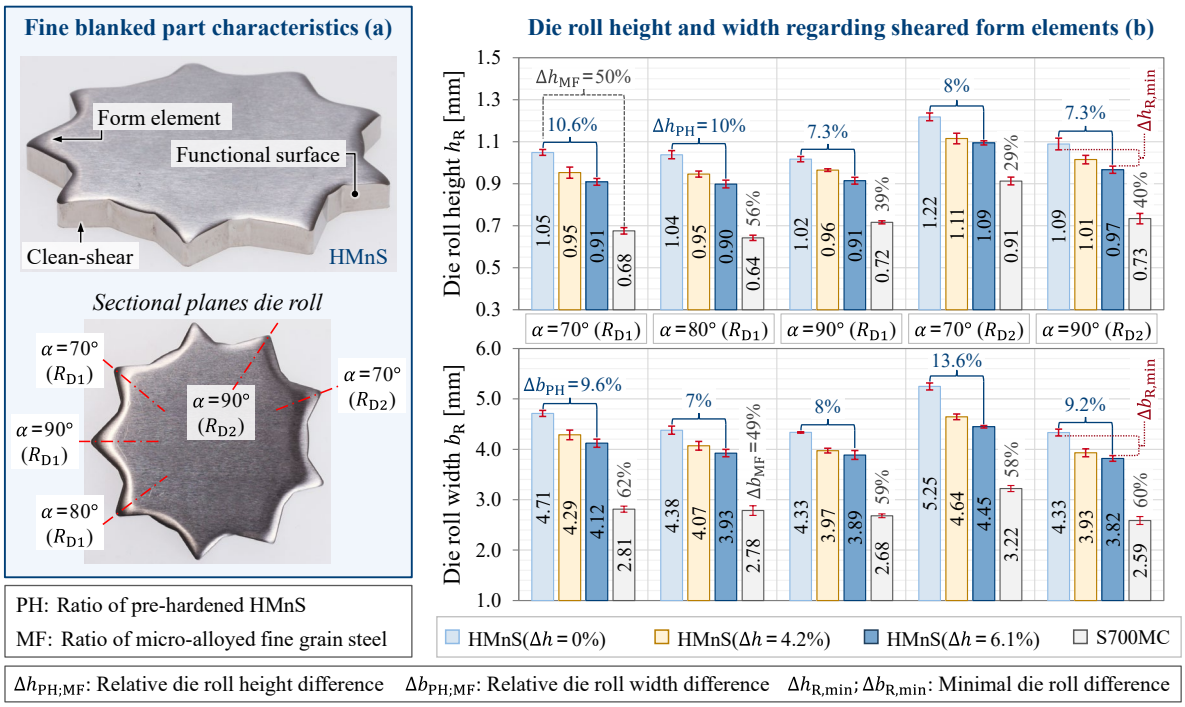

Fig. 7. Characteristics of the investigated fine blanked part (a) and comparison of die roll height width (b).

Regarding the comparison of related relative height reductions Δh of the HMnS, no influence of the tip angle α on the die roll height is observed in terms of the larger tip radius R_{D1} (Fig. 7b). In contrast, a slightly decreasing trend with increasing tip angle is detectable for the die roll width. With respect to the smaller tip radius R_{D2}, the comparison of the relative height reductions for HMnS shows a significant increase in die roll heights and widths with decreasing tip angle. For the S700MC, a comparable behavior to the HMnS is observed for both tip radii with regard to the influence of the tip angle on the die roll height and width.

Discussion and Conclusion on Fine Blanking of Pre-Hardened HMnS

The influence of pre-hardened HMnS X40MnCrAlV19-2 LY on the sheared surface hardening as well as the quality determining attributes during fine blanking was investigated. The process-immanent sheared surface hardening is described in the literature with a positive influence on the wear resistance as well as on the dynamic strengths of tribologically stressed functional surfaces and thus offers the potential to substitute a subsequent heat treatment after fine blanking. The investigated HMnS showed a good formability with high strain hardening during fine blanking, but with regard to the use as lightweight material also exhibits a low yield strength in relation to the tensile strength. In order to increase the strength values, HMnS sheet blanks were pre-hardened by means of flat coining and subsequently fine blanked with an analog geometry representing tribologically stressed functional surfaces (form elements). With almost the same tensile strength compared to the additionally fine blanked HSS S700MC, the hardening properties of HMnS lead to an increase in the maximum blanking force of 6.3% for the reference state and 13.7% for the second pre-hardening stage. Increased blanking forces cause especially at a high difficulty level D increased tool loads during fine blanking due to locally high stresses [24] and require the use of

appropriate tool materials regarding a sufficiently high tool life [13]. Compared to the reference state, the relative height reduction of the second pre-hardening stage (Δh = 6.1%) led to a steeper rise of the blanking force progression as well as to a 6.9% increase of the maximum blanking force. Forming-induced strain hardening generally results in an increase in yield as well as tensile strength due to dislocation accumulation and increased dislocation density [9]. This is reflected in the blanking force progression of the second pre-hardening stage of the HMnS, so that an increase in the strengths as well as in the yield strength ratio $R_{\mathrm{p0.2}}/R_{\mathrm{m}}$ can be assumed. The higher strength was also evident in a 20.7% increase in the bulk hardness for the second pre-hardening stage.
Based on the deformation mechanisms, the high strain hardening capacity of HMnS caused an enormous increase in hardness in the near-surface area ($d_S \leq 0.5$ mm) of the functional surfaces compared with HSS S700MC. Directly below the sheared surface, the hardness values increased with increasing blanking path from 500 HV (top) to 630 HV (bottom). Due to the process characteristics of fine blanking, the high deformation of the sheet material in the area in front of the die edge leads to heat dissipation. Based on results in the literature for shearing with a small die clearance [11], a temperature increase in the range of 170 to 210 °C is to be expected with increasing blanking path for the sheet thickness and blanking velocity investigated in this work. The tensile tests of HMnS showed a reduction of the strain hardening curve with a temperature increase in the quasi-static case and a significant increase in adiabatic heating with increasing true strain in the dynamic case. Regarding the calculated SFE of HMnS, the TWIP effect is assumed to be the dominant deformation mechanism for the high hardness increase of the sheared surface. However, due to the superposition of high true strain and high temperature rise with increasing blanking path, an influence on the strain hardening behavior in the shear zone as a result of reduced twinning cannot be excluded.

In terms of tribologically stressed functional surfaces, a non-uniform hardness distribution due to the hardening increase depending on the blanking path represents a disadvantage. One possibility to compensate for this hardness gradient is a strain hardening of the die roll side by means of a subsequent forming operation after fine blanking [8]. The pre-hardening state as well as the tip angle of the form elements had no influence on the hardness values in the near-surface area at the respective investigated position of the functional surface. An influence of local stresses due to the geometry of convex form elements on the sheared surface hardening is therefore not determinable. Based on the comparison to case and surface hardening, limit values of the achievable work hardening depth have been determined for the HMnS used as well as the process parameters applied, which allows a first evaluation of potential applications. Compared to the large tear-off heights during fine blanking of DP and TRIP steels described in previous studies, the investigated functional surfaces showed a high quality despite pre-hardening of the HMnS. The higher die roll of the form elements in comparison to S700MC is due to the lower yield strength ratio of HMnS [9]. The observed die roll reduction with increasing pre-hardening of the HMnS confirms the results of previous works [26].
The investigation on fine blanking of pre-hardened HMnS has shown that a combination of process-immanent high sheared surface hardening and increased yield strength with simultaneous optimal functional surface quality is achievable. Based on an appropriate adaptation of the heat treatment and the rolling process in semi-finished HMnS production [17], there is thus the potential to realize sufficiently high basic strengths with high sheared surface hardening for the implementation of lightweight design strategies by exploiting the deformation mechanisms during fine blanking. In summary, the following conclusions are to be derived:

1. Forming-induced pre-hardening in combination with fine blanking allows a targeted global or local increase in strength and thus an influence on the sheared part properties. The pre-hardening of the investigated HMnS increased the basic strength and reduced the die roll.

2. The superposition of high deformation and compressive stress in the shear zone enables an activation of the deformation mechanisms during fine blanking of HMnS. Compared to HSS S700MC, the investigated HMnS was characterized by a significantly increased sheared surface hardening due to the TWIP effect.
3. The achieved sheared surface hardness in the near-surface area was neither dependent on the pre-hardening state nor on the geometry of the sheared part. Due to the good formability of the investigated HMnS, the fine blanked functional surfaces showed a high sheared surface quality despite pre-hardening.
4. Semi-finished HMnS production designed for fine blanking offers the potential to realize application-specific sheared part properties in terms of high functional surface hardness, quality and basic strength by exploiting the deformation mechanisms.

Acknowledgement
The Authors would like to thank *thyssenkrupp Hohenlimburg GmbH* for providing the sheet materials investigated and the *Steel Institute IEHK of RWTH Aachen University* for characterizing the high manganese steel as well as supporting the interpretation of the results.

References
[1] K. Salonitis, P. Ball, Energy Efficient Manufacturing from Machine Tools to Manufacturing Systems, Procedia CIRP 7 (2013) 634-639. https://doi.org/10.1016/j.procir.2013.06.045
[2] L. Cabernard, S. Pfister, S. Hellweg, Improved sustainability assessment of the G20's supply chains of materials, fuels, and food, Environ. Res. Lett. 17 (2022) 34027. https://doi.org/10.1088/1748-9326/ac52c7
[3] S. Rosenthal, F. Maaß, M. Kamaliev, M. Hahn, S. Gies, A.E. Tekkaya, Lightweight in Automotive Components by Forming Technology, Automot. Innov. 3 (2020) 195-209. https://doi.org/10.1007/s42154-020-00103-3
[4] M. Kolbe, Stamping Practice, Springer Fachmedien Wiesbaden, Wiesbaden, 2022.
[5] K. Gupta, N.K. Jain, R. Laubscher, Advances in Gear Manufacturing, in: K. Gupta et al. (Eds.), Advanced Gear Manufacturing and Finishing, Elsevier, 2017, pp. 67-125.
[6] W. Volk, J. Stahl, Shear Cutting, in: T.I.A.f. Produ, L. Laperrière, G. Reinhart (Eds.), CIRP Encyclopedia of Production Engineering, Springer, Berlin, Heidelberg, 2015, pp. 1-9.
[7] U. Aravind, U. Chakkingal, P. Venugopal, A Review of Fine Blanking: Influence of Die Design and Process Parameters on Edge Quality, J. Mater. Eng. Perform. 30 (2021) 1-32. https://doi.org/10.1007/s11665-020-05339-y
[8] R.-A. Schmidt, Cold forming and Fineblanking, Carl Hanser Verlag, Munich, 2007.
[9] F. Klocke, Manufacturing Processes 4: Forming, Springer, Berlin, Heidelberg, 2013.
[10] N. Hatanaka, K. Yamaguchi, N. Takakura, Finite element simulation of the shearing mechanism in the blanking of sheet metal, J. Mater. Process. Technol. 139 (2003) 64-70. https://doi.org/10.1016/S0924-0136(03)00183-3
[11] P. Demmel, In-situ Temperaturmessung beim Scherschneiden. Dissertation, Munich, 2014.
[12] H. Hoffmann, Handbuch Umformen, Hanser Verlag, München, 2012.
[13] H. Voigts, T. Bergs, Investigation of Failure Mechanisms of Cemented Carbide Fine Blanking Punches by Means of Process Forces and Acoustic Emission, in: G. Daehn et al. (Eds.), Forming the Future, Springer International Publishing, Cham, 2021, pp. 1173-1187.
[14] S. Walzer, M. Liewald, Novel approach to decrease sheet thinning during sheet metal forming by using embossing technique, Procedia Manuf. 50 (2020) 795-799. https://doi.org/10.1016/j.promfg.2020.08.143
[15] C. Busch, A. Hatscher, M. Otto, S. Huinink, M. Vucetic, C. Bonk, A. Bouguecha, B.-A. Behrens, Properties and Application of High-manganese TWIP-steels in Sheet Metal Forming, Procedia Eng. 81 (2014) 939-944. https://doi.org/10.1016/j.proeng.2014.10.121

[16] B.C. de Cooman, Y. Estrin, S.K. Kim, Twinning-induced plasticity (TWIP) steels, Acta Mater. 142 (2018) 283-362. https://doi.org/10.1016/j.actamat.2017.06.046
[17] S. Wesselmecking, M. Haupt, Y. Ma, W. Song, G. Hirt, W. Bleck, Mechanism-controlled thermomechanical treatment of high manganese steels, Mater. Sci. Eng. A 828 (2021) 142056. https://doi.org/10.1016/j.msea.2021.142056
[18] A.M. Beese, D. Mohr, Effect of stress triaxiality and Lode angle on the kinetics of strain-induced austenite-to-martensite transformation, Acta Mater. 59 (2011) 2589-2600. https://doi.org/10.1016/j.actamat.2010.12.040
[19] S. Sun, A. Zhao, Q. Wu, Effect of strain rate on the work-hardening rate in high-Mn steel, Mater. Sci. Technol. 33 (2017) 1306-1311. https://doi.org/10.1080/02670836.2017.1288690
[20] A. Saeed-Akbari, J. Imlau, U. Prahl, W. Bleck, Derivation and Variation in Composition-Dependent Stacking Fault Energy Maps Based on Subregular Solution Model in High-Manganese Steels, Metall. Mater. Trans. A 40 (2009) 3076-3090. https://doi.org/10.1007/s11661-009-0050-8
[21] S. Thipprakmas, Improving wear resistance of sprocket parts using a fine-blanking process, Wear 271 (2011) 2396-2401. https://doi.org/10.1016/j.wear.2010.12.015
[22] D. Müller, J. Stahl, A. Nürnberger, R. Golle, T. Tobie, W. Volk, K. Stahl, Shear cutting induced residual stresses in involute gears and resulting tooth root bending strength of a fineblanked gear, Arch. Appl. Mech. 91 (2021) 3679-3692. https://doi.org/10.1007/s00419-021-01915-3
[23] P.J. Zhao, Z.H. Chen, C.F. Dong, Experimental and numerical analysis of micromechanical damage for DP600 steel in fine-blanking process, J. Mater. Process. Technol. 236 (2016) 16-25. https://doi.org/10.1016/j.jmatprotec.2016.05.002
[24] M.D. Gram, R.H. Wagoner, Fineblanking of high strength steels: Control of material properties for tool life, J. Mater. Process. Technol. 211 (2011) 717-728. https://doi.org/10.1016/j.jmatprotec.2010.12.005
[25] E. Spišák, J. Majerníková, E. Spišáková, The Influence of Punch-Die Clearance on Blanked Edge Quality in Fine Blanking of Automotive Sheets, MSF 818 (2015) 264-267. https://doi.org/10.4028/www.scientific.net/MSF.818.264
[26] F. Schweinshaupt, T. Herrig, T. Bergs, Investigation of Combined Flat Coining and Fine Blanking of 16MnCr5 to Influence the Die Roll Formation, in: B.-A. Behrens et al. (Eds.), Production at the Leading Edge of Technology, Springer International Publishing, Cham, 2022, pp. 112-121. https://doi.org/10.1007/978-3-030-78424-9_13
[27] W. Bleck, I. Schael, Determination of crash-relevant material parameters by dynamic tensile tests, Steel Res. 71 (2000) 173-178. https://doi.org/10.1002/srin.200005709
[28] W. Bleck, New insights into the properties of high-manganese steel, Int. J. Miner. Metall. Mater. 28 (2021) 782-796. https://doi.org/10.1007/s12613-020-2166-1